Accepted Manuscript

Design, synthesis and evaluation of 6-aryl-indenoisoquinolone derivatives dual targeting ERα and VEGFR-2 as anti-breast cancer agents

Zhichao Tang, Chengzhe Wu, Tianlin Wang, Kejing Lao, Yejun Wang, Linyi Liu, Moses Muyaba, Pei Xu, Conghui He, Guoshun Luo, Zhouyang Qian, Shaoxiong Niu, Lijun Wang, Ying Wang, Hong Xiao, Qidong You, Hua Xiang

PII: S0223-5234(16)30322-1

DOI: 10.1016/j.ejmech.2016.04.029

Reference: EJMECH 8544

To appear in: *European Journal of Medicinal Chemistry*

Received Date: 21 February 2016

Revised Date: 10 April 2016

Accepted Date: 11 April 2016

Please cite this article as: Z. Tang, C. Wu, T. Wang, K. Lao, Y. Wang, L. Liu, M. Muyaba, P. Xu, C. He, G. Luo, Z. Qian, S. Niu, L. Wang, Y. Wang, H. Xiao, Q. You, H. Xiang, Design, synthesis and evaluation of 6-aryl-indenoisoquinolone derivatives dual targeting ERα and VEGFR-2 as anti-breast cancer agents, *European Journal of Medicinal Chemistry* (2016), doi: 10.1016/j.ejmech.2016.04.029.

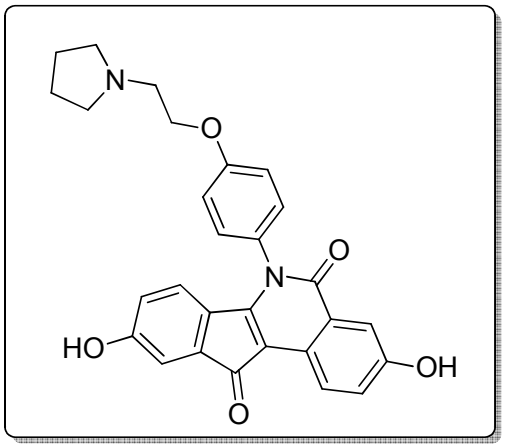

21c

ERα and VEGFR-2 dual inhibitor

ERα IC_{50} = 7.2 μM

VEGFR-2 IC_{50} = 0.099 μM

Anti-proliferation against breast cancer

Raf-1/MAPK/ERK pathway inhibition

Design, synthesis and evaluation of 6-aryl-indenoisoquinolone derivatives dual targeting ERα and VEGFR-2 as anti-breast cancer agents

Zhichao Tang[a,b], Chengzhe Wu[a,b], Tianlin Wang[a,b], Kejing Lao[a,b], Yejun Wang[a,b], Linyi Liu[a,b], Moses Muyaba[a,b], Pei Xu[a,b], Conghui He[a,b], Guoshun Luo[a,b], Zhouyang Qian[a,b], Shaoxiong Niu[a,b], Lijun Wang[c], Ying Wang[c], Hong Xiao[c], Qidong You[a,b], Hua Xiang[a,b,]*.

[a]*Jiangsu Key Laboratory of Drug Design and Optimization, China Pharmaceutical University, 24 Tongjiaxiang, Nanjing 210009, PR China*

[b]*Department of Medicinal Chemistry, School of Pharmacy, China Pharmaceutical University, 24 Tongjiaxiang, Nanjing 210009, PR China*

[c]*Nanjing Brain Hospital Affiliated to Nanjing Medical University, 264 Guangzhou Road, Nanjing 210029, PR China*

Corresponding author

*Tel.: +86 025 83271096; Fax: +86 025 83271096; E-mail: xianghua@cpu.edu.cn(H. Xiang).

Abstract

The estrogen receptors have played important roles in breast cancer development and progression. Selective estrogen receptor modulators, such as Tamoxifen, have showed great benefits in the treatment and prevention of breast cancer. But the disadvantages of induction of endometrial cancer and drug resistance have limited their use. Multiple ligand which act at multiple biomolecular targets may exert favorable advantages of improved efficacy with lower incidence of side effects. In this work, we described the synthesis and evaluation of a series of 6-aryl-indenoisoquinolone derivatives as dual ERα and VEGFR-2 inhibitors. These compounds presented good ERα binding affinity and ERα antagonistic activity, as well as potent VEGFR-2 inhibitory potency. They also possessed excellent anti-proliferative activities against MCF-7, MDA-MB-231, Ishikawa and HUVEC cell lines. Further investigation of selective compound **21c** showed that it was able to inhibit the activation of VEGFR-2 and the signaling transduction of Raf-1/MAPK/ERK pathway in MCF-7 cells.

Keywords: Estrogen receptor; VEGFR-2; Dual inhibitor; Breast cancer.

1. Introduction

Breast cancer (BC) is the most frequent cancer among women worldwide. It had been estimated that 1.67million new cases of BC were diagnosed in 2012 over the world according to WHO report [1]. The estrogen receptors ERα and ERβ which are ligand regulated transcription factors that mediate estrogen activity in many important physiological processes play vital roles in breast cancer development and progression [2,3]. More than 70% breast cancers are estrogen receptor alpha (ERα) positive and estrogen dependent [4]. Endocrine therapy which aims to block the ER transcription effect is regarded as an effective treatment. Thus ERα has provided an ideal pharmaceutical target and a lot of ERα ligands have been developed as antagonists against ERα positive breast cancer [5]. Selective estrogen receptor modulators (SERMs) are a special group of ligands which act as antagonists in breast tissue but agonists in other tissues such as cardiovascular system and bone [6,7]. Due to their special action mode, SERMs remain as important anti-breast cancer agents with benefits in cardiovascular system and maintaining bone density compared with aromatase inhibitors and pure anti-estrogens [8,9]. Tamoxifen is the first

SERM and is currently widely used in the treatment and prevention of breast cancer with solid efficacy documented in several randomized clinical trials [10,11]. Tamoxifen (Figure 1) structurally contains a triphenylethylene scaffold and a basic side chain. Since then, a lot of SERMs with various scaffolds mimicking Tamoxifen were developed for the treatment or prevention of breast cancer [12,13]. Many alternative scaffolds for ER modulators have also been reported, e.g., the heterocyclic propylpyrazoletriol (PPT), *exo*-5,6-bis(4-hydroxyphenyl)-7-oxabicyclo[2.2.1]hept-5-ene-2-sulfonic acid phenyl ester (OBHS) and *m*-carborane-containing compound (Figure 1) [14-16].

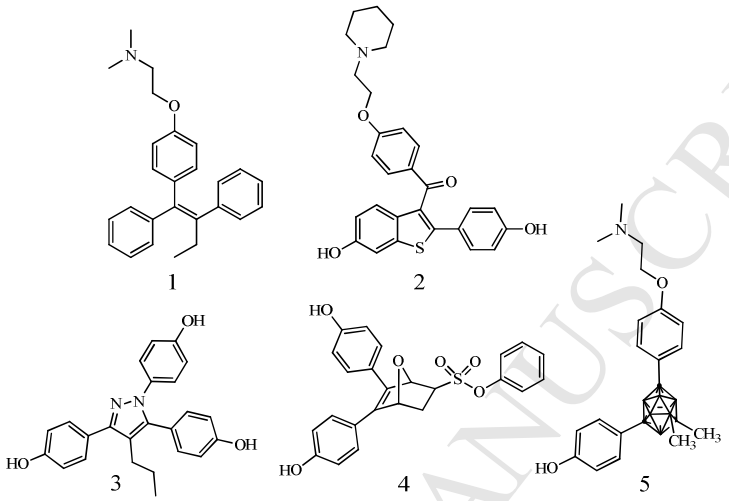

Figure 1. Estrogen receptor ligands: (1) Tamoxifen; (2) Raloxifene; (3) PPT; (4) OBHS; (5) *m*-carborane SERM.

Although SERMs have shown great benefits in treating ERα positive BC, they still remain disadvantages. For example, long-term treatment of Tamoxifen increases the occurrence of endometrial cancer [17]. And another common deficiency that limits the use of SERMs is intrinsic and acquired drug resistance, in which breast tumors become refractory to endocrine therapies and relapse [18,19]. Therefore, the project to develop a SERM with increased activity and less side effects still draws much attention. Multiple ligand is a single chemical entity which acts at multiple biomolecular targets. Designed multiple ligands may exert favorable advantages of improved efficacy and lower incidence of side effects [20]. It has been an attractive way to design multiple ligands in the development of anti-cancer agents [21]. Several studies have shown their multiple ligands toward ER and another target (such as aromatase, HDAC and tubulin) in the discovery of novel anti-breast cancer agents (Figure 2) [22-24].

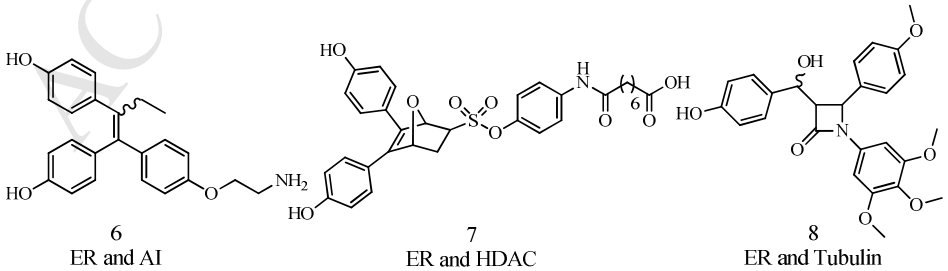

Figure 2. Multiple ligands targeting ER.

We have previously reported a series of 2, 3-diaryl isoquinolinone derivatives as multiple ligands of ERα and vascular endothelial growth factor receptor-2 (VEGFR-2) as anti-breast cancer agents which showed inhibition on the both targets [25]. VEGFR-2 is a member of the receptor

tyrosine kinase (RTK) family and the predominant effector of VEGF/VEGFR signaling in promoting angiogenesis [26]. VEGFR-2 inhibitors were reported in the treatment of breast cancer but are not sufficient as single therapy [27]. However, the combination of Tamoxifen with Brivanib, a VEGFR-2 inhibitor, was reported not only to maximize therapeutic efficacy but also to retard SERM resistant tumour growth [28]. The phosphorylation of VEGFR-2 will activate the Raf-1/MAPK/ERK signaling which is very important for cell proliferation. Moreover, the Raf-1/MAPK/ERK interplayes with ER in regulating estrogen-dependent gene expression and is reported to be involved in the resistance of endocrine therapy [29-31]. It is supposed that a multiple ligand of ER and VEGFR-2 may exhibite inhibition on both ER and MAPK pathways, thus possessing enhanced activity against BC with less disadvantages.

As our ongoing interest to explore different scaffold structures as multiple ligands of ER and VEGFR-2, we designed a series of 6-aryl-indenoisoquinolone derivatives with basic side chain (Table 1). Herein, the synthesis and biological evaluation of the designed compounds were described. They were evaluated for ERα binding affinity, cancer cell anti-proliferative activity, VEGFR-2 inhibition and anti-angiogenesis activity, besides, a selective compound was further investigated for its action mechanism and the molecular modeling was also performed to explore the potential binding mode.

Table 1. Structures of designed compounds

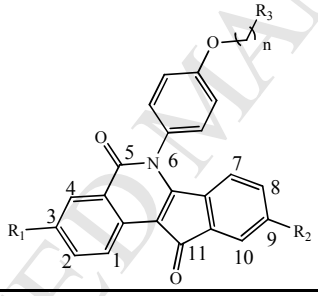

Compound	R_1	R_2	n	R_3
19a	OCH_3	OCH_3	2	
19b	OCH_3	OCH_3	2	
19c	OCH_3	OCH_3	2	
19d	OCH_3	OCH_3	2	
19e	OCH_3	OCH_3	2	
19f	OCH_3	OCH_3	2	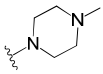
20a	OCH_3	OCH_3	3	
20b	OCH_3	OCH_3	3	

20c	OCH_3	OCH_3	3	
20d	OCH_3	OCH_3	3	
20e	OCH_3	OCH_3	3	
20f	OCH_3	OCH_3	3	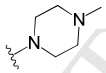
21a	OH	OH	2	
21b	OH	OH	2	
21c	OH	OH	2	
21d	OH	OH	2	
21e	OH	OH	2	
21f	OH	OH	2	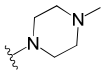

2. Results and discussion

2.1. Chemistry.

The intermediate, 4-methoxyhomophthalic acid **12**, was prepared from commercially available 3-methoxybenzoic acid according to literature procedure in high yields [32]. The synthesis of indenoisoquinolone is usually achieved through a key intermediate of tetrahydroisoquinolone. The cyclodehydration of **12** in toluene and acetic anhydride gave **13**. At the same time, anisaldehyde **14** and p-aminophenol **15** were condensed in ethanol to afford imine **16**. Anhydride **13** and imine **16** were then condensed in acetonitrile catalyzed by $KAl(SO_4)_2 \cdot 12H_2O$ to give tetrahydroisoquinoline-4-carboxylic acid **17** using reported conditions [33]. Compound **18** was then prepared from **17** by chloridization-dehydrogenation and intramolecular Friedel-Crafts reactions (Scheme 2). Combination of different side chains with compound **18** afforded the target compounds **19a-f** and **20a-f**. Compounds **21a-f** were prepared from their corresponding 3,9-dimethoxy compounds **19a-f** by demethylation with BBr_3 (Scheme 3).

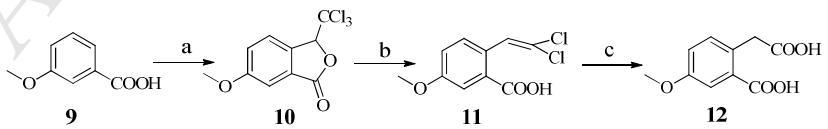

Scheme 1. Synthesis of compound **12**. Reagents and conditions: (a) Chloral hydrate, conc. H_2SO_4, rt, 12h, 83.6 %; (b) Zn, HOAc, rt, 30min; 93.6% (c) Conc. H_2SO_4, rt, 30min, 90%.

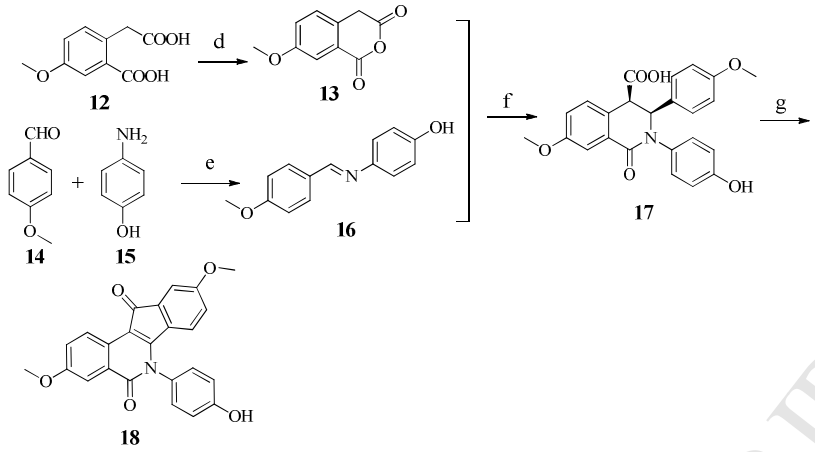

Scheme 2. Synthesis of **18**. Reagents and conditions: (d) acetic anhydride, toluene, reflux, 4h, 100%; (e) ethanol, reflux, 10h, 96.9%; (f) $KAl(SO_4)_2 \cdot 12H_2O$, acetonitrile, rt, 8h, 45.9%; (g) 1) $SOCl_2$, toluene, reflux, 2h; 2) $AlCl_3$, CH_2Cl_2, rt, 10h, 86.7%.

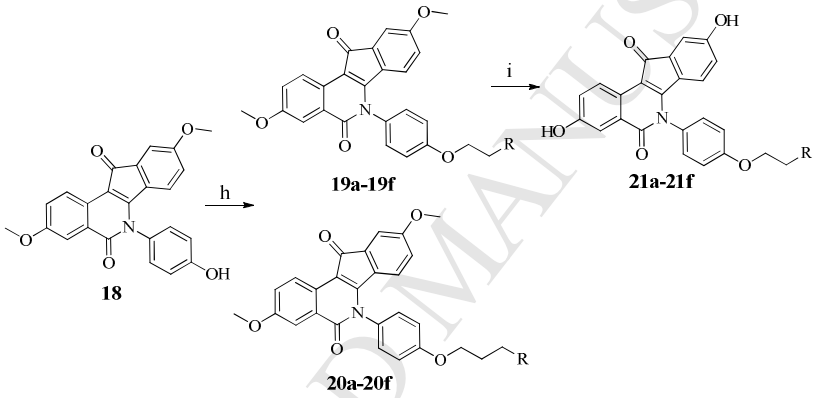

Scheme 3. Synthesis of **19a-f**, **20a-f** and **21a-f**. Reagents and conditions: (h) RCH_2CH_2Cl or $RCH_2CH_2CH_2Cl$, 20% sodium hydroxide, TBAB, THF, reflux, 4h, 37-72%; (i) BBr_3, CH_2Cl_2, rt, 3h, 49-63%.

2.2. Biological evaluation.

2.2.1. ERα binding affinity assay.

The ERα binding affinities of synthesized compounds were initially assessed by following a fluorescence polarization procedure. Tamoxifen was used as the positive control. Results are shown in Table 2. The data can be analyzed in two groupings, compounds **19a-f** and **20a-f**, which bearing two methoxyl group with variations in the basic side chain and compounds **21a-f** with two hydroxyl group. It's obviously to note that compounds **21a-f** possess better binding affinity than the other two series. As is known that the hydrogen bonds formed between the two hydroxyl group of estradiol and Glu353, Arg394 and His524 contribute a lot to keep the conformation stable when estradiol binds to ERα [34]. The ability to form hydrogen bonds with these three key amino acids is widely accepted to identify ERα ligands. The dihydroxyl compounds **21a-f** showed about 3 fold greater binding affinity than the corresponding dimethoxyl compounds **19a-f**. It could be inferred that compounds **21a-f** containing two hydroxyl groups to mimic estradiol were able to form more hydrogen bonds with ERα than methoxyl substituted compounds **19a-f**, thus presenting

better binding affinities. The length of the basic side chain was taken into consideration to explore the influence on binding affinity. In the antagonist binding mode, the terminal amino group pointed toward and formed hydrogen bond with Asp351 to stabilize the conformation. Compounds **19a-f** with two carbon atoms showed slightly better activity than **20a-f** with three carbon atoms in the side chain, which was consistent with the other known SERMs. Different amino substituents were also investigated, among the more potent compounds **21a-f**, it seemed that the bulkier group (morpholinyl, N-methyl piperazinyl) were inferior to the others. Morpholinyl side chain containing compound **21e** showed the lowest binding affinity of 19.8 μM, it was unexpected that compound **19e** and **20e** which possessed two methoxyl group but contain morpholinyl exerted no binding activity. Piperidyl, diethylamine and pyrrolidinyl were more preferable in the side chain. **21d** with piperidyl as the basic group was the most potent compound with an IC_{50} of 3.4μM which is very close to Tamoxifen (IC_{50}=1.0μM).

Table 2 Binding affinity of synthesized compounds for ERα

compound	IC_{50}(μM)	compound	IC_{50}(μM)
19a	24.4	20d	38.3
19b	18.7	20e	>100
19c	17.7	20f	35.2
19d	24.9	21a	7.6
19e	>100	21b	6.7
19f	23.3	21c	7.2
20a	39.4	21d	3.4
20b	39.8	21e	19.8
20c	40.3	21f	10.6
Tamoxifen	1.0		

2.2.2. Cancer cells anti-proliferative activity.

To evaluate the anticancer activity, all synthesized compounds were screened against human breast cancer cell line MCF-7 (ER+), MDA-MB-231 (ER-) and human endometrial cancer cell line Ishikawa. It is known that Tamoxifen will stimulate endometrial cell growth and induce endometrial cancer after long term treatment, it is of concern to evaluate the influence of new compounds targeting ER on endometrial cells. Results are summarized in Table 3. Tamoxifen was used as the positive control in breast cancer cells .

As a global observation, most of the synthesized compounds presented significant antiproliferative activity on these three cancer cell lines. Moreover, the active compounds demonstrated better activity in breast cancer than in endometrial cancer cells, and most of them were more active than Tamoxifen in the two breast cancer cells. As for ER+ and ER- breast cancer cells, the compounds could inhibit their growth on the same degree which indicated that the antiproliferative activity was acquired not only through ERα but a multi-target effect. Compounds with morpholinyl group in the side chain which showed no binding affinity in ERα assay were also not active in this test because the IC_{50} values of compound 1**9e**, **20e** and **21e** were not determined up to the highest concentrations tested, which indicated an ERα pathway on the antiproliferative activity. The N-methyl piperazinyl compound **20f** with three carbon atoms in the side chain also showed no activity while compound **19f** which has two carbon atoms in the side

chain showed no activity only on MDA-MB-231, although compound **19f** and **21f** showed activity but yet were less potent in their group. The bulkier basic group were still unfavourable in suppressing cancer cell growth.

The most potent compound against MCF-7 was **19d** with an IC_{50} of 0.3μM, about 18 fold more potent than Tamoxifen (5.3μM), but only showed moderate activity compared with other compounds against MDA-MB-231 and Ishikawa with the IC_{50} valued at 2.8μM and 9.6μM respectively. It was interesting to find that dimethoxyl compounds (**19a**, **19b**, **19c**, **19d** and **19f**) which were less potent in ERα binding assay manifested slightly greater potency than the corresponding dihydroxyl compounds (**21a**, **21b**, **21c**, **21d** and **21f**) against MCF-7 which also confirmed that the obtained antiproliferative activity was not only through ERα. However, this preference was inversed in Ishikawa cells, the dihydroxyl group showed the best activity and the most active compound **21b** gave an IC_{50} of 4.0μM. Similar to Ishikawa, the dihydroxyl group also present better activity against MDA-MB-231 except **21a** which showed a decrease compared with **19a** and **20a**. The most potent compound was **21c** with an IC_{50} of 0.5μM, exhibiting 27 fold greater potency than Tamoxifen (13.9μM).

Investigation on the length of the side chain revealed an unfavorite in longer side chain in MCF-7 and a decrease in activity was observed (**20a** vs **19**a, **20b** vs **19b**, **20c** vs **19c** and **20d** vs **19d**). Similar trend was seen in MDA-MB-231 (**20b** vs **19b**, **20c** vs **19c** and **20d** vs **19d**) but no such conclusion can be summarized based on the data of Ishikawa.

Analysis of the influence of different basic group on antiproliferative activity suggested a preference for three medium size basic group, diethylamine, pyrrolidinyl and piperidyl (**19b**, **19c**, **19d**, **21b**, **21c** and **21d**). For example, **19d**, the most potent compound against MCF-7, was piperidyl substituted, and **21c** against MDA-MB-231 was pyrrolidinyl substituted while **21b** against Ishikawa was diethylamine substituted. Overall, compounds with shorter side chain and the above three basic groups displayed the best activity against all of the three cancer cell lines.

Table 3 Cancer cells antiproliferative activity (IC_{50}, μM)

compound	MCF-7	MDA-MB-231	Ishikawa
19a	1.1	1.1	10.6
19b	0.7	1.3	6.7
19c	0.7	0.7	8.7
19d	0.3	2.8	9.6
19e	>100	>100	>100
19f	1.1	>100	10.9
20a	1.4	0.6	9.6
20b	2.3	1.5	4.1
20c	3.2	3.0	12.8
20d	7.8	21.7	4.5
20e	>100	>100	>100
20f	>100	>100	>100
21a	3.8	3.3	5.1
21b	0.8	1.0	4.0
21c	1.2	0.5	8.2
21d	1.1	0.8	4.3

21e	>100	>100	>100
21f	2.5	4.1	6.1
Tamoxifen	5.3	13.9	6.0

2.2.3. Antiangiogenic activity evaluation.

This evaluation was carried out by assessing VEGFR-2 inhibitory activity and HUVEC anti-proliferative activity. Results are summarized in Table 4 and Figure 1. As shown in Table 4, six compounds manifested inhibition on VEGFR-2 (**19a**, **19b**, **21a**, **21b**, **21c**, **21d**). The dihydroxyl group compounds were also preferable for VEGFR-2 inhibition. The most potent compounds **21b** and **21c** were equipotent to the positive control Sunitinib. The IC_{50} values of **21b** and **21c** were 0.12μM and 0.099μM respectively while Sunitinib possessed an IC_{50} of 0.14μM in our test. These six compounds presented significant antiproliferative activity against HUVEC as well. Compound **21c** which showed best activity on VEGFR-2 was also the most potent one against HUVEC with the IC_{50} of 0.8μM, same with that of Sunitinib. When the dimethoxyl group was changed into dihydroxyl group (**19a** vs **21a**, **19b** vs **21b**), an increase on VEGFR-2 inhibition by roughly ten fold was observed. It was found that medium size basic groups were superior to others because when it changed from dimethylamine to diethylamine, the inhibition on VEGFR-2 was increased by about 3 fold (**19a** vs **19b**, **21a** vs **21b**), this is especially true for **21c** which showed the greatest potency possesses an five-member ring pyrrolidinyl. As the direct effect of VEGFR-2 inhibition, similar changes on activity against HUVEC proliferation were observed. However, other five compounds (**19f**, **20a**, **20b**, **20c**, **21f**) which were inactive in VEGFR-2 assay also showed noteworthy inhibition on HUVEC proliferation indicating another mechanism for their acquired activity.

The inhibitory effect of the most potent compound **21c** on VEGFR-2 was further determined by assessing the phosphorylation level of VEGFR-2 in HUVEC cells using western blot. As shown in Figure 3, **21c** was able to block the phosphorylation of VEGFR-2 in a dose dependent manner. Sunitinib was used as the positive control. At the concentration of 1μM, **21c** was equipotent to Sunitinib and showed no statistically significant difference ($P > 0.05$).

Based on the above results, **21c** showed excellent activities on the both targets and was chosen as dual inhibitor candidate for further investigation.

Table 4 Antiangiogenic activity on VEGFR-2 and HUVEC

compound	VEGFR-2	HUVEC
19a	3.9	35.6
19b	1.03	11.4
19c	NA	>100
19d	NA	>100
19e	NA	>100
19f	NA	12.0
20a	NA	25.0
20b	NA	16.0
20c	NA	5.1
20d	NA	>100
20e	NA	>100

20f	NA	>100
21a	0.33	4.6
21b	0.12	1.8
21c	0.099	0.8
21d	0.25	1.3
21e	NA	>100
21f	NA	1.1
Sunitinib	0.14	0.8

NA = not active.

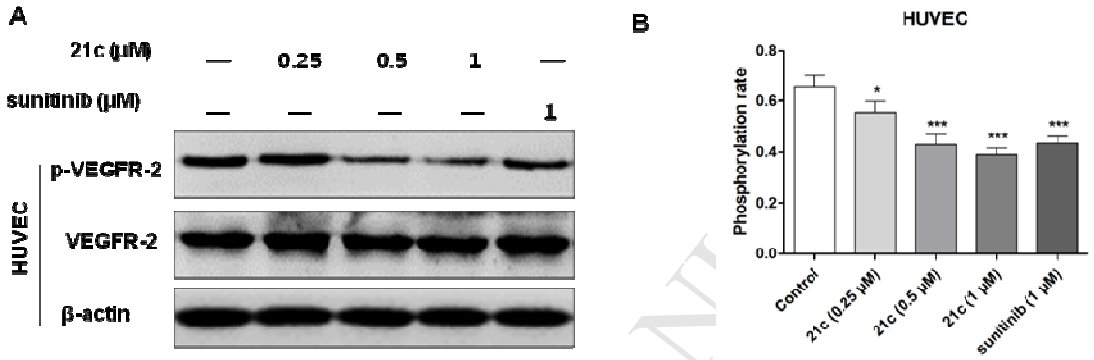

Figure 3. 21c inhibits the phosphorylation of VEGFR-2 in HUVEC cells. Expression of p-VEGFR-2 and VEGFR-2 in HUVEC cells were examined by western blots. Densitometric analysis was performed to determine the phosphorylation rate of VEGFR-2. Values are mean ±SD (n=3). * $P < 0.05$, ** $P < 0.01$, *** $P < 0.001$ vs. Control group.

2.2.4. Effect of 21c on the expression of progestrone receptor microRNA in MCF-7 cells.

To assess the pharmacological properties of the test compound on estrogen responsive genes, we used real-time polymerase chain reaction (RT-PCR) in the ER positive MCF-7 cells to evaluate the modulation of progesterone receptor (PgR). The progesterone receptor expression is commonly used to assess estrogenic or antiestrogenic activity. As shown in Figure 4, presence of 10 nM estradiol (E2) was able to remarkably elevate the mRNA expression of PgR gene compared to the vehicle control. The mRNA expression level of PgR with 10nM E2 was regard as 100%. Tamoxifen was used as the positive control at the concentration of 1μM in combination with 10nM E2 and could reduce the expression of PgR mRNA by about seventy percent. Compound **21c** exhibited stronger antagonism against the expression of PgR mRNA than Tamoxifen at the concentration of 1μM in the presence of 10nM E2 and showed statistically significant difference compared to Tamoxifen, indicating that **21c** presented significantly antiestrogenic property.

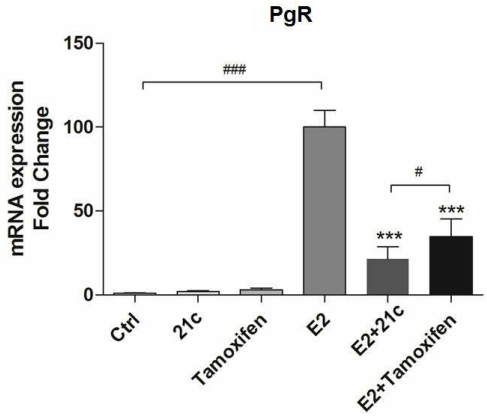

Figure 4. The increased mRNA expression of PgR induced by E2 was reversed by **21c** in MCF-7 cells. The mRNA expression of PgR was examined by Real-time PCR. Values are mean ±SD (n=5). * $P < 0.05$, ** $P < 0.01$, *** $P < 0.001$ vs. E2 group. $^{\#}P < 0.05$, $^{\#\#}P < 0.01$, $^{\#\#\#}P < 0.001$.

2.2.5. 21c inhibits the MAPK signaling cascade as the result of VEGFR-2 phosphorylation blockade in MCF-7 cells.

The Raf-1/MAPK/ERK pathway is an important cell signaling pathways and controls multiple cellular processes, such as cell proliferation and differentiation [35]. Increased activity of the Ras/Raf-1/MAPK pathway plays an important role in the development and progression and is one of the hallmarks of more aggressive cancers. Over activation of Raf-1/MAPK pathway is also involved in the endocrine resistance [31]. The inhibition of Raf-1/MAPK/ERK pathway is supposed to enhance the effect of anti-hormonal therapy and retard endocrine resistance. Compound **21c** has shown its inhibition on VEGFR-2 in the antiagiogenesis evaluation, we made further investigation of **21c** on inhibiting VEGFR-2 activation and the Raf-1/MAPK/ERK pathway transduction in MCF-7 cells to explore its dual-target effect. As shown in Figure 5 and Figure 6, **21c** was able to inhibit the activation of VEGFR-2 in MCF-7 cells as like in HUVEC. We then investigated how **21c** affected the Raf-1/MAPK/ERK pathway, two effectors, Raf-1 and ERK were examined. As expected, result showed an inhibition on this pathway as their activation was suppressed in the presence of **21c** or Sunitinib. And there is no statistically significant difference between **21c** and Sunitinib at the concentration of 1μM ($P > 0.05$). This synergetic inhibitory effect of **21c** on ERα and VEGFR-2 suggested it as an promising dual-target agent against breast cancer.

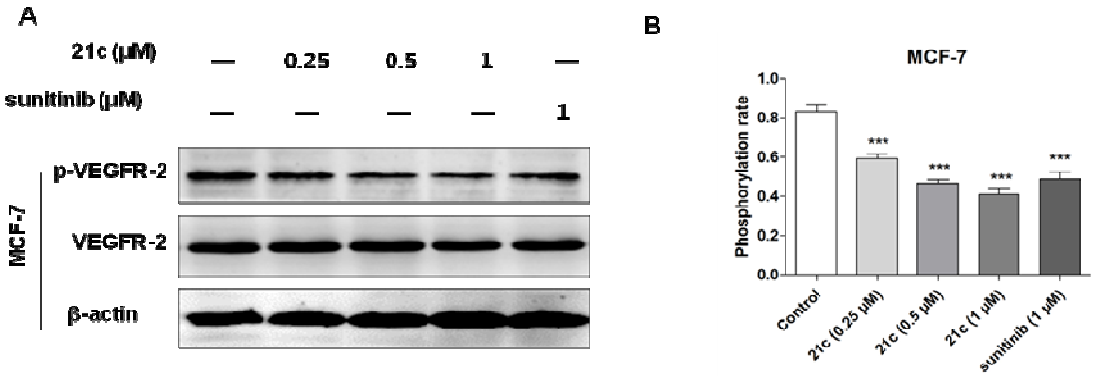

Figure 5. 21c inhibits the phosphorylation of VEGFR-2 in MCF-7 cells. (A) Expression of p-VEGFR-2 and VEGFR-2 in MCF-7 cells were examined by western blots. (B) Densitometric analysis was performed to determine the phosphorylation rate of VEGFR-2. Values are mean ±SD (n=3). * $P < 0.05$, ** $P < 0.01$, *** $P < 0.001$ vs. Control group.

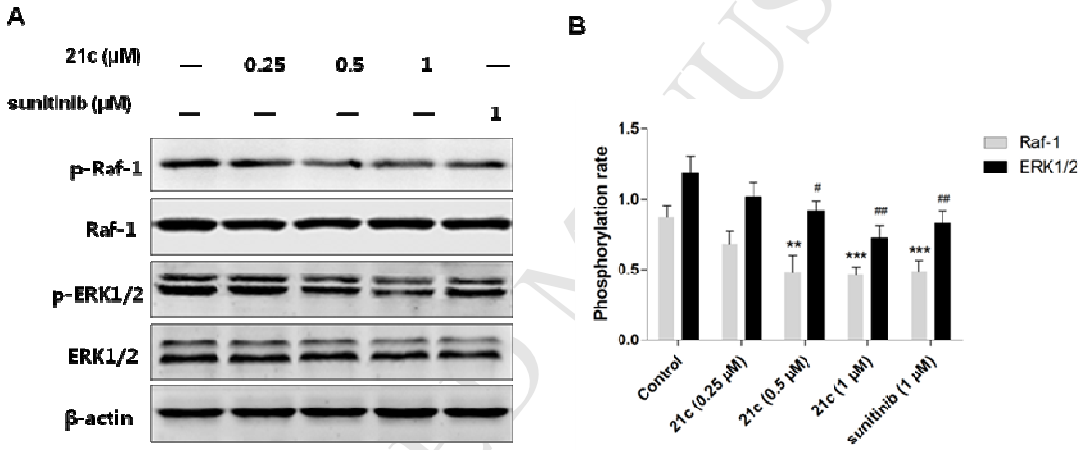

Figure 6. 21c inhibits the activity of the Raf-1/ERK pathway in MCF-7 cells. (A) Expression of p-Raf-1, Raf-1, p-ERK1/2, and ERK1/2 were examined by western blots in MCF-7 cells. (B) Densitometric analysis was performed to determine the phosphorylation rate of Raf-1 and ERK1/2 . Values are mean ±SD (n=3). * $P < 0.05$, ** $P < 0.01$, *** $P < 0.001$ vs. Control group; $^{\#}$ $P < 0.05$, $^{\#\#}$ $P < 0.01$, $^{\#\#\#}$ $P < 0.001$ vs. Control group.

2.3. Molecular modeling.

We performed docking studies to explore the potential binding mode of the dual targeting compound **21c** in ERα and VEGFR-2. Results are shown in Figure 7. **21c** was favorably docked into the binding site of ERα. The 9-OH of **21c** interacted with Glu353 and Arg394 which mimic the A-ring phenol of estradiol while the 3-OH interacted with His524 which mimic the 17-OH of estradiol. The basic side chain of **21c** pointed toward Asp351 to generate an antagonistic conformation as that of 4-OHT. The binding orientation of **21c** within the ligand binding domain of VEGFR-2 showed a binding mode which was different with Sunitinib but similar to that of diaryl urea VEGFR-2 inhibitors. The skeleton occupied the ATP region while 9-OH formed hydrogen bonds with two amino acid residues in the hinge region, Glu915 and Cys917 which played important roles in the interaction of VEGFR-2 and its ligands. The side chain of **21c** pointed toward a hydrophobic region which was commonly occupied by the diaryl urea fragment.

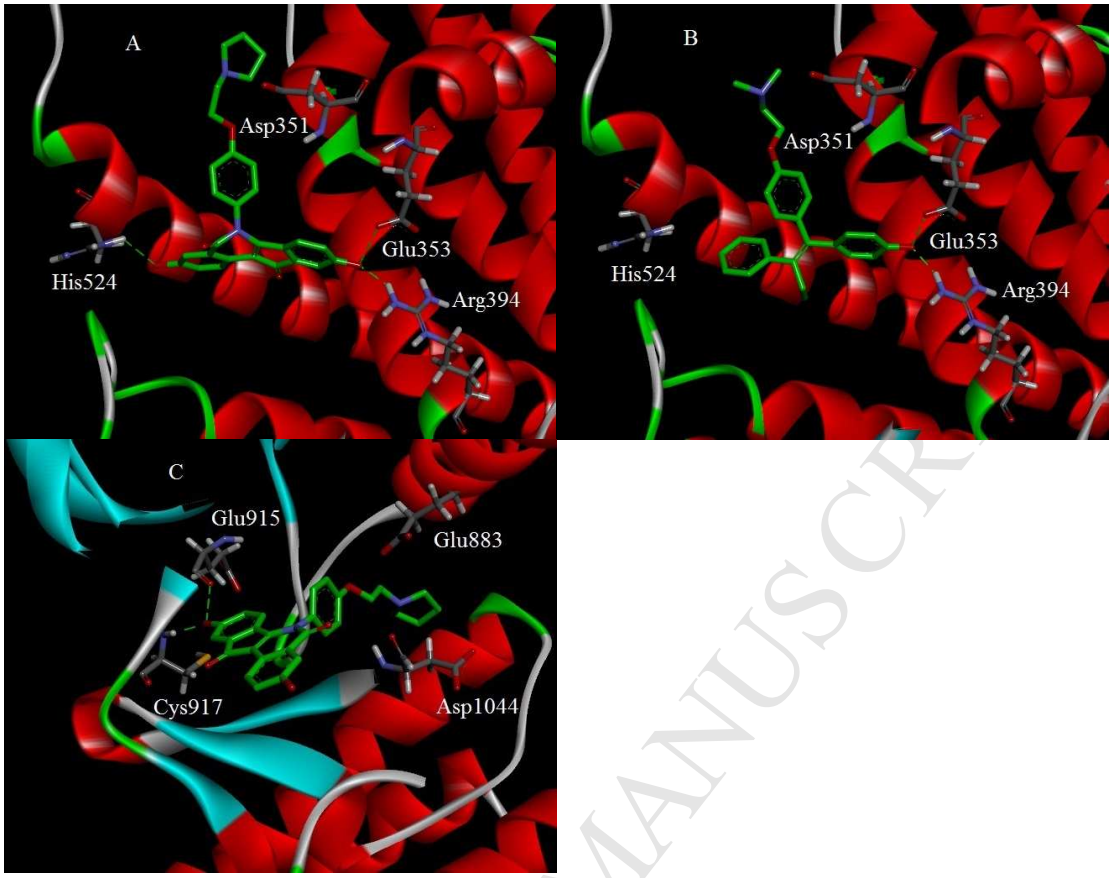

Figure 7. (A) Predicted binding mode of **21c** within the LBD of ERα (PDB ID: 3ERT). (B) Binding mode of 4-OH-Tamoxifen within the LBD of ERα (PDB ID: 3ERT). (C) Predicted binding mode of **21c** within the LBD of VEGFR-2 (PDB ID: 1YWN).

3. Conclusion

To explore different scaffold structures as dual ligands of ERα and VEGFR-2, we have designed and synthesized a series of 6-aryl-indenoisoquinolone derivatives with basic side chain. Most of them presented good inhibitory activities toward ERα with excellent anti-proliferative activities against three cancer cell lines, some of them showed potent VEGFR-2 inhibitory activity. Compound **21c** was found to be the most potential inhibitor on the both targets, further evaluation revealed that **21c** was able to inhibit the activation of VEGFR-2 and the signaling transduction of Raf-1/MAPK/ERK pathway in MCF-7 cells. **21c** was therefore a promising dual targeting candidate for the development of anti-breast cancer agents. These results also suggested a new and potential route in the discovery of drugs against breast cancer.

4. Experimental section

4.1. Chemistry

4.1.1. General.

Most chemicals and solvents were of analytical grade and, when necessary, were purified and dried by standard methods. Reactions were monitored by thin-layer chromatography (TLC) using precoated silica gel plates (silica gel GF/UV 254), and spots were visualized under UV light (254 nm). Melting points (uncorrected) were determined on a Mel-TEMP II melting point apparatus and are uncorrected. Infrared (IR) spectra (KBr) were recorded on a Nicolet Impact 410 instrument (KBr pellet). ^{1}H NMR and ^{13}C NMR spectra were recorded with a Bruker Avance 300 MHz spectrometer at 300 K, using TMS as an internal standard. MS spectra were recorded on a

Shimadzu GC–MS 2050 (ESI) or an Agilent 1946A-MSD (ESI) Mass Spectrum, or a LC/MSD TOF HR-MS Spectrum. Column chromatography was performed with silica gel (100-200 mesh). Chemical shifts (d) are expressed in parts per million relative to tetramethylsilane, which was used as an internal standard, coupling constants (J) are in hertz (Hz), and the signals are designated as follows: s, singlet; d, doublet; t, triplet; m, multiplet; brs, broad singlet.

4.1.2. General method I: S_N2 reaction.

A suspension of compound 18 (0.4g, 1mmol), alkyl chlorides (2.5mmol), TBAB (0.1mmol) in THF (5mL) was stirred at room temperature. A solution of NaOH (0.2g, 5mmol) in water (1mL) was added. The mixture was heated to reflux for 4h under nitrogen. The reaction mixture was poured into ice water (25mL). The precipitated product was collected by filtration, and further purified by silica gel column chromatography to afford the final product.

4.1.3. General method II: demethylation of 6-arylindenoisoquinolone derivatives.

A solution of 6-arylindenoisoquinolone derivatives (0.4mmol) in dry CH_2Cl_2 (10mL) was cooled to -30^{o}C by cryotrap. A solution of BBr_3 (2.4mmol) in dry CH_2Cl_2 (2.4mL) was added dropwise under nitrogen. The mixture was gently warmed to room temperature and stirred for 3h. The reaction mixture was quenched with H_2O (50mL), then saturated sodium bicarbonate solution was added to pH=8. The precipitate was collected by filtration, and further purified by silica gel column chromatography to afford the demethylation product.

*4.1.4. 3-Trichloromethyl-6-methoxy-1(3H)-isobenzofuranone (**10**).* 3-Methoxylbenzonic acid (5g, 32.9mmol) was dissolved in concentrated sulfuric acid (20mL) and chloral hydrate (6.5g, 39.5mmol) was added. After reacting for 12h at room temperature, the mixture was poured onto ice (100g), and the precipitated product was collected by filtration, washed with saturated sodium bicarbonate solution and water to pH=7, air-dried to give crude product (9.1g) which was stirred in ethanol (36.4ml) for 4 h, filtrated and air-dried to give pure compound **10** (7.7g, 83.6%); mp 128-130^{o}C (ref: 132-134^{o}C); MS (ESI, m/z): 282 $[M+H]^+$.

*4.1.5. 2-(β, β-Dichloroethenyl)-5-methoxybenzoic acid (**11**).* Compound **10** (1g, 3.55mmol) was firstly added in glacial acetic acid (5mL) and zinc dust (0.46g, 7.1mmol) was added in small portions. The reaction mixture was stirred for 30 minutes at room temperature, and then heated to reflux for 5minutes. The hot solution was immediately filtered and cooled to room temperature to give white needle-shaped crystals. The crystals were collected by filtration and the filtrate was poured into ice water (25mL). The precipitate was collected, air-dried and recrystallized with acetic acid. Two parts of crystals were combined to give compound **11** (0.82g, 93.6%); mp 163-165^{o}C (ref: 166-168^{o}C); MS (ESI, m/z): 246 $[M-H]^-$.

*4.1.6. (2-Carboxy-4-methoxy)-phenyl acetic acid (**12**).* Compound **11** (0.6g, 2.3mmol) was dissolved in concentrated sulfuric acid (1.8mL). The mixture was stirred for 30 minutes at room temperature and poured onto ice (5g). The precipitated product was filtered, washed with cold water and purified by recrystallization from a mixed acetone/H_2O solution (acetone:H_2O; 3:1) to yield compound **12** as white solid (0.4g, 90%); mp 187-189^{o}C; MS (ESI, m/z): 209 $[M-H]^-$.

*4.1.7. 7-Methoxyisochroman-1,3-dione (**13**).* An mixture of compound **12** (2.0g, 11.1mmol), acetic anhydride (2.1mL, 22.2mmol) and toluene (20mL) was refluxed at 120 ^{o}C for 4 h. The solvent was reduced in vacuo to give compound **13** as light yellow solid (1.82g, 100.0%); mp 136-138 ^{o}C; MS (ESI, m/z): 193 $[M+H]^+$.

*4.1.8. 4-((4-Methoxybenzylidene)-amino)-phenol (**16**).* A mixture of 4-aminophenol (5g, 45.4mmol), 4-methoxybenzaldehyde (5.6ml, 45.4mmol) in ethanol (50ml) was refluxed at 80 ^{o}C

for 2 h under an inert atmosphere. The reaction mixture was cooled to room temperature, and precipitated product was collected by filtration to yield compound **16** as light yellow solid (10g, 96.9%); mp 182-184 ^{o}C; MS (ESI, m/z): 228 $[M+H]^{+}$.

4.1.9.

*(3S,4R)-2-(4-Hydroxyphenyl)-7-methoxy-3-(4-methoxyphenyl)-1-oxo-1,2,3,4-tetrahydroisoquinoline-4-carboxylic acid (**17**).* Compound **13** (4.5g, 23.4mmol) was dissolved in acetonitrile (100ml), then compound **16** (5.3g, 23.4mmol) and $KAl(SO_4)_2 \cdot 12H_2O$ (5.54g, 11.7mmol) were added to the solution. The mixture was stirred at room temperature for 8 h. Half of the acetonitrile was evaporated in vacuo. The crude product was collected by filtration, washed successively with acetonitrile and chloroform. The yellow product was stirred in water until it became a uniform suspension, filtrated to afford light yellow solid. The pure compound **17** was prepared by stirring in methanol to give a white solid (4.5g, 45.9%); mp 158-160 ^{o}C; ^{1}H NMR (300MHz, DMSO-d_6) δ 9.47 (s, 1H), 6.65-7.56 (m, 11H, Ar-H), 5.25 (d, *J*=5.7Hz, 1H), 4.83 (d, *J*=5.4Hz, 1H), 3.83 (s, 3H), 3.65 (s, 3H); MS (ESI, m/z): 418 $[M-H]^{-}$.

*4.1.10. 3,9-Dimethoxy-6-(4-hydroxyphenyl)-5H-indeno[1,2-c]isoquinoline-5,11(6H)-dione (**18**).* Compound **17** (4.5g, 10.7mmol) was suspended in toluene (45 mL), and thionyl chloride (15.6ml, 214mmol) was added dropwise. Then the mixture was heated to reflux for 2h. The solvent was removed in vacuo and the remaining was dissolved in dry dichloromethane (45ml). Aluminum chloride (2.87g, 21.4mmol) was added into the solution after cooled to 0 ^{o}C by an external ice bath. After reacting for 10 h at room temperature, the reaction mixture was poured into a solution of ice water (200mL) and concentrated hydrochloric acid (9mL). The oil layer was separated and stirred with ethanol (100mL). Compound **18** was given by filtration as red solid (3.7g, 86.7%); mp >300 ^{o}C; ^{1}H NMR (300MHz, DMSO-d_6) δ 5.40-8.45 (m, 10H, Ar-H), 3.86 (s, 3H), 3.74 (s, 3H); MS (ESI, m/z): 400 $[M+H]^{+}$.

4.1.11.

*3,9-Dimethoxy-6-(4-(2-(dimethylamino)ethoxy)phenyl)-5H-indeno[1,2-c]isoquinoline-5,11(6H)-dione (**19a**).* Compound **19a** was prepared from **18** and 2-chloro-N,N-dimethylethanamine hydrochloride as red solid according to general method I (0.32g, 68.6%); mp 190-193 ^{o}C; IR (KBr) 3069, 2951, 2755, 1668, 1510, 1255, 1059, 788, 526 cm^{-1}; ^{1}H NMR (300MHz, DMSO-d_6) δ 5.32-8.40 (m, 10H, Ar-H), 4.19 (t, *J*=5.5 Hz, 2H), 3.83 (s, 3H), 3.71 (s, 3H), 2.78 (t, 2H), 2.32 (s, 6H). ^{13}C NMR (75MHz, DMSO-d_6) δ 189.17, 162.43, 161.52, 159.12, 154.02, 136.83, 130.03, 129.77, 128.28, 126.37, 124.22, 124.10, 123.69, 123.18, 115.35, 115.12, 110.40, 108.81, 106.29, 65.78, 57.38, 55.75, 55.38, 45.26; MS (ESI, m/z): 471 $[M+H]^{+}$; Anal. Calcd for $C_{28}H_{26}N_2O_5$: C, 71.47; H, 5.57; N, 5.95. Found: C, 71.09; H, 5.74; N, 5.64.

4.1.12.

*3,9-Dimethoxy-6-(4-(2-(diethylamino)ethoxy)phenyl)-5H-indeno[1,2-c]isoquinoline-5,11(6H)-dione (**19b**).* Compound **19b** was prepared from **18** and 2-chloro-N,N-diethylethanamine hydrochloride as red solid according to general method I (0.34g, 68.3%); mp 169-172 ^{o}C; IR (KBr) 3445, 2929, 1666, 1508, 1248, 1058, 1026,790 cm^{-1}; ^{1}H NMR (300MHz, $CDCl_3$) δ 5.44-8.51 (m, 10H, Ar-H), 4.17 (t, *J*=6.0 Hz, 2H), 3.88 (s, 3H), 3.76 (s, 3H), 2.96 (t, *J*=6.0 Hz, 2H), 2.71 (q, *J*=7.1 Hz, 4H), 1.13 (t, *J*=7.1 Hz, 6H). ^{13}C NMR (75MHz, $CDCl_3$) δ 189.52, 163.09, 161.26, 159.26, 157.93, 154.23, 136.84, 129.61, 128.98, 128.36, 126.51, 124.37, 124.10, 123.71, 122.86, 115.19, 114.62, 109.93, 108.23, 107.23, 66.67, 55.15, 55.00, 51.20, 47.52, 11.35; MS (ESI, m/z): 499 $[M+H]^{+}$; Anal. Calcd for $C_{30}H_{30}N_2O_5 \cdot 0.5H_2O$: C, 70.98; H, 6.16; N, 5.52. Found: C, 70.53; H,

6.14; N, 5.36.

4.1.13.

*3,9-Dimethoxy-6-(4-(2-(pyrrolidin-1-yl)ethoxy)phenyl)-5H-indeno[1,2-c]isoquinoline-5,11(6H)-dione (**19c**).* Compound **19c** was prepared from **18** and 1-(2-chloroethyl)pyrrolidine hydrochloride as red solid according to general method I (0.36g, 72.6%); mp 171-174 ^{o}C; IR (KBr) 3432, 2926, 1663, 1509, 1246, 1057, 790, 600 cm^{-1}; ^{1}H NMR (300MHz, $CDCl_3$) δ 5.42-8.50 (m, 10H, Ar-H), 4.24 (t, *J*=5.6 Hz, 2H), 3.87 (s, 3H), 3.75 (s, 3H), 3.00 (t, *J*=5.6 Hz, 2H), 2.70 (t, 4H), 1.86 (m, 4H). ^{13}C NMR (75MHz, $CDCl_3$) δ 189.53, 163.08 161.25, 159.22, 157.90, 154.20, 136.81, 129.68, 129.00, 128.37, 126.48, 124.35, 124.07, 123.69, 122.83, 115.24, 114.56, 109.96, 108.20, 107.21, 67.04, 55.15, 54.99, 54.59, 54.40, 23.02; MS (ESI, m/z): 497 $[M+H]^+$; Anal. Calcd for $C_{30}H_{28}N_2O_5 \cdot 0.4H_2O$: C, 71.53; H, 5.76; N, 5.56. Found: C, 71.36; H, 5.67; N, 5.53.

4.1.14.

*3,9-Dimethoxy-6-(4-(2-(piperidin-1-yl)ethoxy)phenyl)-5H-indeno[1,2-c]isoquinoline-5,11(6H)-dione (**19d**).* Compound **19d** was prepared from **18** and 1-(2-chloroethyl)piperidine hydrochloride as red solid according to general method I (0.33g, 64.7%); mp 98-100 ^{o}C; IR (KBr) 3437, 2943, 1663, 1509, 1246, 1057, 790, 600 cm^{-1}; ^{1}H NMR (300MHz,$CDCl_3$) δ 5.43-8.49 (m, 10H, Ar-H), 4.23 (t, *J*=5.9 Hz, 2H), 3.87 (s, 3H), 3.75 (s, 3H), 2.86 (t, *J*=5.9 Hz, 2H), 2.57 (brs, 4H), 1.65 (m, 4H), 1.49 (m, 2H). ^{13}C NMR (75MHz, $CDCl_3$) δ 189.50, 163.07 161.25, 159.21, 157.91, 154.19, 136.82, 129.67, 129.01, 128.34, 126.48, 124.35, 124.08, 123.67, 122.81, 115.25, 114.56, 109.93, 108.23, 107.29, 65.98, 57.43, 55.13, 54.98, 54.71, 25.42, 23.66; MS (ESI, m/z): 511 $[M+H]^+$; Anal. Calcd for $C_{31}H_{30}N_2O_5 \cdot 0.8H_2O$: C, 70.92; H, 6.07; N, 5.34. Found: C, 70.47; H, 6.05; N, 5.34.

4.1.15.

*3,9-Dimethoxy-6-(4-(2-morpholinoethoxy)phenyl)-5H-indeno[1,2-c]isoquinoline-5,11(6H)-dione (**19e**).* Compound **19e** was prepared from **18** and 4-(2-chloroethyl)morpholine hydrochloride as red solid according to general method I (0.28g, 54.7%); mp 97-100 ^{o}C; IR (KBr) 3457, 2959, 1666, 1510, 1248, 1116, 1025, 572 cm^{-1}; ^{1}H NMR (300MHz,$CDCl_3$) δ 5.46-8.57 (m, 10H, Ar-H), 4.25 (t, *J*=5.6Hz, 2H), 3.90 (s, 3H), 3.78-3.81 (m, 7H), 2.90 (t, *J*=5.6Hz, 2H), 2.66 (t, *J*=4.3Hz, 4H). ^{13}C NMR (75MHz, $CDCl_3$) δ 189.59, 163.13 161.33, 159.09, 158.01, 154.17, 136.90, 129.82, 129.05, 128.35, 126.54, 124.44, 124.14, 123.81, 122.78, 115.25, 114.65, 110.04, 108.27, 107.55, 66.43, 65.77, 57.14, 55.20, 55.05, 53.71; MS (ESI, m/z): 513 $[M+H]^+$; HRMS (ESI) for $C_{30}H_{28}N_2O_6$+H calcd 513.2020, found 513.2015.

4.1.16.

*3,9-Dimethoxy-6-(4-(2-(4-methylpiperazin-1-yl)ethoxy)phenyl)-5H-indeno[1,2-c]isoquinoline-5,11(6H)-dione (**19f**).* Compound **19f** was prepared from **18** and 1-(2-chloroethyl)-4-methylpiperazine hydrochloride as red solid according to general method I (0.31g, 59.0%); mp 204-208 ^{o}C; IR (KBr) 3477, 2934, 2791, 1664, 1509, 1305, 1245, 1058, 789, 606 cm^{-1}; ^{1}H NMR (300MHz,$CDCl_3$) δ 5.41-8.46 (m, 10H, Ar-H), 4.23 (t, *J*=5.6Hz, 2H), 3.86 (s, 3H), 3.73 (s, 3H), 2.91 (t, *J*=5.6Hz, 2H), 2.69 (brs, 4H), 2.53 (brs, 4H), 2.32 (s, 3H). ^{13}C NMR (75MHz, $CDCl_3$) δ 189.48, 163.06 161.23, 159.11, 157.88, 154.14, 136.78, 129.75, 129.04, 128.30, 126.45, 124.32, 124.04, 123.67, 122.78, 115.21, 114.52, 109.93, 108.18, 107.28, 65.85, 56.62, 55.13, 54.97, 54.51, 53.15, 45.54; MS (ESI,m/z): 526 $[M+H]^+$; Anal. Calcd for $C_{31}H_{31}N_3O_5$: C, 70.84; H, 5.94; N, 7.99. Found: C, 70.40; H, 5.99; N, 7.70.`

4.1.17. 3,9- Dimethoxy

-6-(4-(3-(dimethylamino)propoxy)phenyl)-5H-indeno[1,2-c]isoquinoline-5,11(6H)-dione ***(20a)***. Compound **20a** was prepared from **18** and 3-chloro-N,N-dimethylpropan-1-amine hydrochloride as red solid according to general method I (0.21g, 43.4%); mp 178-180 ^{o}C; IR (KBr) 3415, 2934, 1665, 1407, 1247, 1057, 790, 605 cm^{-1}; ^{1}H NMR (300MHz, DMSO-d_6) δ 5.34-8.42 (m, 10H, Ar-H), 4.12 (t, *J*=6.3Hz, 2H), 3.84 (s, 3H), 3.72 (s, 3H), 2.46 (t, *J*=6.3Hz, 2H), 2.19 (s, 6H), 1.92 (m, 2H). ^{13}C NMR (75MHz, DMSO-d_6) δ 189.62, 162.43 161.54, 159.37, 157.90, 155.04, 136.84, 129.87, 129.75, 128.30, 126.39, 124.53, 124.12, 123.69, 123.195, 115.29, 115.11, 110.44, 108.84, 106.04, 66.21, 55.76, 55.57, 55.40, 45.08, 26.72; MS (ESI, m/z): 485 [M+H]$^{+}$; Anal. Calcd for $C_{29}H_{28}N_2O_5$: C, 71.88; H, 5.82; N, 5.78. Found: C, 71.57; H, 6.03; N, 5.54.

4.1.18. 3,9-Dimethoxy-6-(4-(3-(diethylamino)propoxy)phenyl)-5H-indeno[1,2-c]isoquinoline-5,11(6H)-dione ***(20b)***. Compound **20b** was prepared from **18** and 3-chloro-N,N-diethylpropan-1-amine hydrochloride as red solid according to general method I (0.19g, 37.1%); mp 144-146 ^{o}C; IR (KBr) 3412, 2934, 1667, 1510, 1249, 1058, 790, 604 cm^{-1}; ^{1}H NMR (300MHz,$CDCl_3$) δ 5.42-8.51 (m, 10H, Ar-H), 4.17 (t, 2H), 3.87 (s, 3H), 3.74 (s, 3H), 2.89-2.99 (m, 6H), 2.19 (m, 2H), 1.26 (t, *J*=6.5Hz, 6H). ^{13}C NMR (75MHz, $CDCl_3$) δ 189.56, 163.11, 161.28, 159.12, 157.93, 154.23, 136.79, 129.82, 129.10, 128.27, 126.50, 124.38, 124.06, 123.74, 122.79, 115.11, 114.48, 110.13, 108.20, 107.21, 65.54, 55.19, 55.01, 48.57, 46.14, 24.77, 9.65; MS (ESI, m/z): 513 [M+H]$^{+}$; HRMS for $C_{31}H_{32}N_2O_5$+H calcd 513.2384, found 513.2380.

4.1.19. 3,9-Dimethoxy-6-(4-(3-(pyrrolidin-1-yl)propoxy)phenyl)-5H-indeno[1,2-c]isoquinoline-5,11(6H)-dione ***(20c)***. Compound **20c** was prepared from **18** and 1-(3-chloropropyl)pyrrolidine hydrochloride as red solid according to general method I (0.21g, 41.2%); mp 200-204 ^{o}C; IR (KBr) 3428, 2925, 1663, 1509, 1247, 1057, 790, 604 cm^{-1}; ^{1}H NMR (300MHz,$CDCl_3$) δ 5.43-8.47 (m, 10H, Ar-H), 4.15 (t, *J*=6.2Hz, 2H), 3.86 (s, 3H), 3.73 (s, 3H), 2.60-2.74 (m, 6H), 2.11 (m, 2H), 1.84 (m, 4H). ^{13}C NMR (75MHz, $CDCl_3$) δ 189.51, 163.08, 161.21, 159.37, 157.86, 154.23, 136.78, 129.50, 129.10, 128.32, 126.46, 124.32, 124.04, 123.67, 122.89, 115.15, 114.49, 109.93, 108.15, 107.25, 66.26, 55.13, 54.98, 53.81, 52.63, 28.24, 22.96; MS (ESI,m/z): 511[M+H]$^{+}$; Anal. Calcd for $C_{31}H_{30}N_2O_5 \cdot 0.4H_2O$: C, 71.91; H, 5.99; N, 5.41. Found: C, 71.45; H, 5.71; N, 5.35.

4.1.20. 3,9-Dimethoxy-6-(4-(3-(piperidin-1-yl)propoxy)phenyl)-5H-indeno[1,2-c]isoquinoline-5,11(6H)-dione ***(20d)***. Compound **20d** was prepared from **18** and 1-(3-chloropropyl)piperidine hydrochloride as red solid according to general method I (0.21g, 40%); mp 200-204 ^{o}C; IR (KBr) 3415, 2938, 1163, 1509, 1246, 1058, 790, 604 cm^{-1}; ^{1}H NMR (300MHz,$CDCl_3$) δ 5.45-8.51 (m, 10H, Ar-H), 4.14 (t, *J*=6.2Hz, 2H), 3.88 (s, 3H), 3.75 (s, 3H), 2.47-2.59 (m, 6H), 2.09 (m, 2H), 1.64 (m, 4H), 1.45 (m, 2H). ^{13}C NMR (75MHz, $CDCl_3$) δ 189.55, 163.11, 161.26, 159.41, 157.92, 154.22, 136.84, 129.50, 129.09, 128.98, 126.50, 124.37, 124.10, 123.71, 122.83, 115.11, 114.54, 110.00, 108.22, 107.21, 66.43, 55.43, 55.16, 55.01, 54.18, 26.23, 25.40, 23.87; MS (ESI, m/z): 525 [M+H]$^{+}$; HRMS for $C_{32}H_{32}N_2O_5$+H calcd 525.2384, found 525.2381.

4.1.21. 3,9-Dimethoxy-6-(4-(3-morpholinopropoxy)phenyl)-5H-indeno[1,2-c]isoquinoline-5,11(6H)-dione ***(20e)*** . Compound **20e** was prepared from **18** and 4-(3-chloropropyl)morpholine hydrochloride as red solid according to general method I (0.2g, 38.0%); mp 224-226 ^{o}C; IR (KBr) 3049, 2943, 1662, 1508, 1246, 1056, 790, 603 cm^{-1}; ^{1}H NMR (300MHz,$CDCl_3$) δ 5.45-8.50 (m, 10H, Ar-H) , 4.16 (t,

J=6.2Hz, 2H), 3.88 (s, 3H), 3.75-3.78 (m, 7H,), 2.52-2.63 (m, 6H), 2.07 (m, 2H). ^{13}C NMR (75MHz, $CDCl_3$) δ 189.52, 163.10, 161.26, 159.35, 157.93, 154.18, 136.84, 129.58, 129.02, 128.37, 126.49, 124.37, 124.09, 123.71, 122.79, 115.17, 114.57, 109.94, 108.22, 107.22, 66.49, 66.05, 55.15, 55.00, 54.91, 53.28, 25.90; MS (ESI, m/z): 527 $[M+H]^+$; Anal. Calcd for $C_{31}H_{30}N_2O_6 \cdot 1.2H_2O$: C, 67.92; H, 5.95; N, 5.11. Found: C, 67.46; H, 5.82; N, 4.80.

*4.1.22. 3,9-Dimethoxy-6-(4-(3-(4-methylpiperazin-1-yl)propoxy)phenyl)-5H-indeno[1,2-c]isoquinoline-5,11(6H)-dione (**20f**).* Compound **20f** was prepared from **18** and 1-(3-chloropropyl)-4-methylpiperazine hydrochloride as red solid according to general method I (0.21g, 39.0%); mp 179-182 ^{o}C; IR (KBr) 2959, 2800, 1666, 1510, 1252, 1056, 791, 605 cm^{-1}; ^{1}H NMR (300MHz,$CDCl_3$) δ 5.41-8.44 (m, 10H, Ar-H) , 4.13 (t, *J*=6.2Hz, 2H), 3.86 (s, 3H), 3.71 (s, 3H), 2.56-2.63 (m, 10H), 2.32 (s, 3H), 2.06 (m, 2H). ^{13}C NMR (75MHz, $CDCl_3$) δ 189.42, 163.03, 161.19, 159.34, 157.83, 154.14, 136.77, 129.54, 129.01, 128.30, 126.42, 124.28, 124.02, 123.60, 122.77, 115.14, 114.46, 109.86, 108.15, 107.21, 66.15, 55.10, 54.95, 54.54, 52.59, 45.46, 26.20; MS (ESI, m/z): 540 $[M+H]^+$; HRMS for $C_{32}H_{33}N_3O_5$+H calcd 540.2493 , found 540.2505.

4.1.23.

*3,9-Dihydroxy-6-(4-(2-(dimethylamino)ethoxy)phenyl)-5H-indeno[1,2-c]isoquinoline-5,11(6H)-dione (**21a**).* Compound **21a** was prepared from **19a** as red solid according to general method II (0.1g, 56.4%); mp 186-190 ^{o}C; IR (KBr) 3073, 2922, 1650, 1509, 1246, 1056, 800 cm^{-1}; ^{1}H NMR (300MHz, DMSO-d_6) δ 10.25 (brs, 1H), 10.05 (s, 1H), 5.23-8.35 (m, 10H, Ar-H), 4.15 (t, *J*=5.3Hz, 2H), 2.67 (t, *J*=5.3Hz, 2H), 2.24 (s, 6H). ^{13}C NMR (75MHz, DMSO-d_6) δ 189.66, 162.47, 160.00, 159.10, 156.14, 155.03, 137.04, 130.01, 129.76, 126.83, 125.12, 124.27, 124.09, 123.77, 123.26, 116.64, 115.27, 111.71, 111.15, 106.04, 66.11, 57.59, 45.55; MS (ESI, m/z): 443$[M+H]^+$; HRMS for $C_{26}H_{22}N_2O_5$+H calcd 443.1601, found 443.1597.

4.1.24.

*3,9-Dihydroxy-6-(4-(2-(diethylamino)ethoxy)phenyl)-5H-indeno[1,2-c]isoquinoline-5,11(6H)-dione (**21b**).* Compound **21b** was prepared from **19b** as red solid according to general method II (0.12g, 63.7%); mp 186-190 ^{o}C; IR (KBr) 3070, 2918, 1650, 1507, 1241, 1050, 793 cm^{-1}; ^{1}H NMR (300MHz, DMSO-d_6) δ 10.09 (s, 1H), 5.24-8.36 (m, 10H, Ar-H), 4.26 (t, 2H), 3.11 (t, 2H), 2.83 (q, *J*=7.1Hz, 4H), 1.1 (t, *J*=7.1Hz, 6H). ^{13}C NMR (75MHz, DMSO-d_6) δ 189.65, 162.46, 160.00, 158.77, 156.15, 154.95, 137.02, 130.26, 129.82, 126.80, 125.10, 124.25, 124.11, 123.76, 123.21, 116.58, 115.36, 111.69, 111.17, 106.04, 65.52, 50.75, 47.07, 10.64; MS (ESI, m/z): 471 $[M+H]^+$; HRMS for $C_{28}H_{26}N_2O_5$+H calcd 471.1914 , found 471.1917.

4.1.25.

*3,9-Dihydroxy-6-(4-(2-(pyrrolidin-1-yl)ethoxy)phenyl)-5H-indeno[1,2-c]isoquinoline-5,11(6H)-dione (**21c**).* Compound **21c** was prepared from **19c** as red solid according to general method II (0.13g, 64.0%); mp 186-190 ^{o}C; IR (KBr) 3070, 2920, 1645, 1502, 1241, 1051, 795 cm^{-1}; ^{1}H NMR (300MHz, DMSO-d_6) δ 10.23 (brs, 2H), 5.25-8.37 (m, 10H, Ar-H), 4.19 (t, *J*=5.4Hz, 2H), 2.86 (t, *J*=5.4Hz, 2H), 2.57 (brs, 4H), 1.71 (brs, 4H). ^{13}C NMR (75MHz, DMSO-d_6) δ 189.69, 162.47, 160.15, 159.08, 156.19, 155.02, 137.04, 130.01, 129.76, 126.82, 125.10, 124.25, 124.07, 123.77, 123.25, 116.64, 115.24, 111.70, 111.19, 105.99, 67.04, 54.21, 54.02, 23.11; MS (ESI, m/z): 469 $[M+H]^+$; HRMS for $C_{28}H_{26}N_2O_5$+H calcd 469.2122, found 469.2117.

4.1.26.

3,9-Dihydroxy-6-(4-(2-(piperidin-1-yl)ethoxy)phenyl)-5H-indeno[1,2-c]isoquinoline-5,11(6H)-dio

ne (21d). Compound **21d** was prepared from **19d** as red solid according to general method II (95mg, 49.2%); mp 186-190 ^{o}C; IR (KBr) 3075, 2925, 1650, 1507, 1248, 1053, 801 cm^{-1}; ^{1}H NMR (300MHz, DMSO-d_6) δ 10.09 (brs, 1H), 5.26-8.36 (m, 10H, Ar-H), 4.20 (t, *J*=5.4Hz, 2H), 2.74 (t, *J*=5.4Hz, 2H), 1.35-1.53 (m, 6H). ^{13}C NMR (75MHz, DMSO-d_6) δ 189.63, 162.46, 160.00, 159.09, 156.14, 154.94, 137.02, 130.03, 129.75, 126.80, 125.12, 124.24, 124.08, 123.72, 123.22, 116.60, 115.31, 111.70, 111.14, 106.05, 65.84, 57.20, 54.36, 25.43, 23.79; MS (ESI, m/z): 483 [M+H]$^{+}$; HRMS for $C_{29}H_{26}N_2O_5$+H calcd 483.1914 , found 483.1917.

4.1.27.

3,9-Dihydroxy-6-(4-(2-morpholinoethoxy)phenyl)-5H-indeno[1,2-c]isoquinoline-5,11(6H)-dione (21e). Compound **21e** was prepared from **19e** as red solid according to general method II (0.11g, 58.1%); mp 186-190 ^{o}C; ^{1}H NMR (300MHz, DMSO-d_6) δ 10.29 (s, 1H), 10.06 (s, 1H), 5.26-8.37 (m, 10H, Ar-H), 4.22 (t, *J*=5.7Hz, 2H), 3.61 (t, *J*=4.5Hz, 2H), 2.76 (t, *J*=5.7Hz, 2H), 2.53 (brs, 4H). ^{13}C NMR (75MHz, DMSO-d_6) δ 189.65, 162.47, 159.98, 159.07, 156.14, 154.98, 137.03, 130.05, 129.76, 126.82, 125.12, 124.26, 124.09, 123.74, 123.24, 116.62, 115.31, 111.70, 111.15, 106.03, 66.14, 65.66, 56.94, 53.63; MS (ESI, m/z): 485 [M+H]$^{+}$; HRMS for $C_{29}H_{27}N_3O_5$+H calcd 485.1912, found 485.1916.

4.1.28.

3,9-Dihydroxy-6-(4-(2-(4-methylpiperazin-1-yl)ethoxy)phenyl)-5H-indeno[1,2-c]isoquinoline-5,11 (6H)-dione (21f). Compound **21f** was prepared from **19f** as red solid according to general method II (0.12g, 60.2%); mp 186-190 ^{o}C; ^{1}H NMR (300MHz, DMSO-d_6) δ 5.24-8.36 (m, 10H, Ar-H), 4.19 (t, *J*=5.4Hz, 2H), 2.74 (t, *J*=5.4Hz, 2H), 2.39-2.50 (brs, 8H), 2.19 (s, 3H). ^{13}C NMR (75MHz, DMSO-d_6) δ 189.66, 162.47, 160.02, 159.07, 156.14, 154.98, 137.00, 130.03, 129.75, 126.80, 125.11, 124.24, 124.09, 123.75, 123.24, 116.63, 115.30, 111.68, 111.16, 106.02, 65.85, 56.45, 54.52, 52.82, 45.50; MS (ESI, m/z): 498 [M+H]$^{+}$; HRMS for $C_{29}H_{27}N_3O_5$+H calcd 498.2023, found 498.2034.

4.2. Biological evaluation.

4.2.1. ERα Binding Affinity Assay.

The recombinant ERα (New Durg Screening Center, China Pharmaceutical University, Nanjing, China) and the fluorescent estrogen ligands (self-made) were removed from the -80^{o}C freezer and thawed on ice for 1h prior to use. The fluorescent estrogen ligand was added to the ERα and screening buffer (ES2 Screening Buffer, Invitrogen, USA) was added to make the final concentration 9nM for fluorescent estrogen and 30nM for ERα. Test compounds were accurately weighed and dissolved in DMSO, screening buffer was added to dilute to required concentration. Test compound (1μL) was added to 49μL screening buffer in each well (384-well microplate, Corning, USA). To this 50μL of the fluorescent estrogen/ER complex was added to make up a final volume of 100μL. A positive control contained 50μL estradiol buffer (1nM) and 50μL fluorescent estrogen/ER complex. A negative control contained 50μL screening buffer and 50μL fluorescent estrogen/ER complex. The negative control was used to determine the polarization value when no competitor was present (theoretical maximum polarization). The microplate was incubated in the dark at room temperature for 2 h and shaken on a plate shaker. The polarization values were read on a Safire microplate reader and used to calculate the IC_{50} values.

4.2.2. MTT Assay for Anti-proliferative Activities.

Cells were cultured in RPMI1640 medium (containing 10% (v/v) FBS, 100U/mL Penicillin and 100μg/mL Streptomycin) in a 5% CO_2-humidified atmosphere at 37 ^{o}C. Cells were trypsinized

and seeded at a density of 1×10^5/mL into a 96-well plate (100μL/well) and incubated at 37°C, 5% CO_2 atmosphere for 24 h. After this time they were treated with 100μL/well medium containing test compounds which had been pre-prepared to provide the concentration range of 1×10^{-4}mol/L, 1×10^{-5}mol/L, 1×10^{-6}mol/L and 1×10^{-7}mol/L, and re-incubated for a further 48h. Control wells were added the equivalent volume of medium containing 1% (v/v) DMSO. 20μL MTT (5mg/mL) was added and cells continued to incubate in darkness at 37°C for 4h. The culture medium was then removed carefully and 150μL DMSO was added. The cells were maintained at room temperature in darkness for 20 min to ensure thorough color diffusion before reading the absorbance. The absorbance values were read at 490nm for determination of IC_{50} values.

4.2.3. VEGFR-2 Kinase Inhibitory Assay.

VEGFR-2 kinase assay was conducted using homogeneous time resolved fluorescence (HTRF) assay. The general procedures were as following: VEGFR-2 kinase (Invitrogen, USA), substrates, ATP and test compounds were mixed and incubated in a final buffer with the total volume of 10μL in 384-well microplate. Wells containing the substrate and the kinase without compound were used as total reaction control. The assay plate was incubated at 30°C in the dark for 1 h. Detection was performed with HTRF module of Beckman Coulter detection platform to get the fluorescence values which were further used to calculate the IC_{50} values.

4.2.4. Western Blots.

Cells with different treatments for 24h were washed twice with PBS, then collected and lysed in lysis buffer (100 mM of Tris–Cl, pH 6.8, 4% (m/v) SDS, 20% (v/v) glycerol, 200 mM of β-mercaptoethanol, 1mM of PMSF, 0.1 mM NaF and DTT) for 1 h on the ice. The lysates were then subjected to centrifugation (13,000 rpm) at 4 °C for 20 min. Protein concentration in the supernatants was detected by BCA protein assay (Thermo, Waltham, MA). Then equal amount of protein was separated with 12% SDS-PAGE and transferred to polyvinylidene difluoride (PVDF) membranes (Millipore, Bedford, MA) using a semi-dry transfer system (Bio-rad, Hercules, CA). Proteins were detected using specific antibodies overnight at 4 °C followed by HRP-conjugated secondary antibodies for 1 h at 37 °C. All of the antibodies were diluted in PBST containing 1% BSA. Enhanced chemiluminescent reagents (Beyotime, Jiangsu, China) were used to detect the HRP on the immunoblots, and the visualized bands were captured by film. The bands were quantified by Quantity One software (Vision 4.62, Bio-rad, Hercules, CA), and the relative protein level were normalized to β-actin.

4.2.5. Real-Time Polymerase Chain Reaction (RT-PCR).

RNA samples were reverse transcribed to cDNA and the PCR reactions were performed using TaKaRa SYBR Green Master Mix (Code. no. 638320) carried out in StepOnePlus™ Real-Time PCR instrument (4376600, Life Technologies). The program for amplification was 1 cycle of 95°C for 2 min followed by 40 cycles of 95°C for 10 s, 60°C for 30 s, and 95°C for 10 s. The PCR results were normalized to GAPDH expression and were quantified by the ΔΔCT method.

4.3. Molecular Modeling.

The molecular modeling was performed with Discovery Studio.2.5/CDOCK protocol (*Accelrys Software Inc.*). The crystal structures of ERα complexed with 4-hydroxytamoxifen (PDB code: 3ERT) and VEGFR-2 (PDB code: 1YWN) were downloaded from Protein Data Bank. Compound **21c** was drown and optimized using Hyperchem v7.0. The protein and ligand were optimized and charged with CHARMm force field to perform docking. Up to 30 conformations

were retained, and binding modes presented graphically are representative of the highest-scored conformations.

Supporting Information

^{1}H NMR and ^{13}C NMR spectrum for compounds **19a-21f**.

Acknowledgements

This work was supported by grants from the NSFC (81373279), the Twelfth Five-Year Plan Major Project of Candidate Drugs (Ministry of National Science and Technology, 2012ZX09103101048), the Jiangsu Province Science and Technology Support Program of Social Development Projects (BE2012745) and the Innovation Project of Jiangsu Province.

Abbreviations

BC, breast cancer; ER, estrogen receptor; SERMs, selective estrogen receptor modulators; PPT, propylpyrazoletriol; OBHS, *exo*-5,6-bis(4-hydroxyphenyl)-7-oxabicyclo[2.2.1]hept-5-ene-2-sulfonic acid phenyl ester; AI, aromatase inhibitor; HDAC, histone deacetylases; VEGF, Vascular endothelial growth factor; VEGFR-2, Vascular endothelial growth factor receptor-2; RTK, receptor tyrosine kinase; MAPK, mitogen-activated protein kinase; ERK, extracellular regulated kinases; HUVEC, human umbilical vein endothelial cell; RT-PCR, real-time polymerase chain reaction; PgR, progesterone receptor; E2, estradiol.

References

[1] L.A. Torre, F. Bray, R.L. Siegel, J. Ferlay, J. Lortet-Tieulent, A. Jemal, Global Cancer Statistics, 2012, CA-Cancer J. Clin. 65 (2015) 87-108.

[2] P. Ascenzi, A. Bocedi, M. Marino, Structure-function relationship of estrogen receptor alpha and beta: impact on human health, Mol. Aspects Med. 27 (2006) 299-402.

[3] S. Sommer, S.A.W. Fuqua, Estrogen receptor and breast cancer, Semin. Cancer Biol. 11 (2001) 339-352.

[4] W.F. Anderson, N. Chatterjee, W.B. Ershler, O.W. Brawley, Estrogen receptor breast cancer phenotypes in the surveillance, epidemiology, and end results database, Breast Cancer Res. Treat. 76 (2002) 27-36.

[5] E.A. Ariazi, J.L. Ariazi, F. Cordera, V.C. Jordan, Estrogen receptors as therapeutic targets in breast cancer, Curr. Top. Med. Chem. 6 (2006) 181-202.

[6] V.C. Jordan, Antiestrogens and selective estrogen receptor modulators as multifunctional medicines. 1. Receptor interactions, J. Med. Chem. 46 (2003) 883-908.

[7] V.C. Jordan, Antiestrogens and selective estrogen receptor modulators as multifunctional medicines. 2. Clinical considerations and new agents, J. Med. Chem. 46 (2003) 1081-1111.

[8] B.S. Katzenellenbogen, J.A. Katzenellenbogen, Biomedicine - Defining the "S" in SERMs, Science 295 (2002) 2380-2381.

[9] V.C. Jordan, Chemoprevention of breast cancer with selective oestrogen-receptor modulators, Nat. Rev. Cancer 7 (2007) 46-53.

[10] M. Clarke, R. Collins, C. Davies, J. Godwin, R. Gray, R. Peto, E.B.C.T.C. Grp, Tamoxifen for early breast cancer: An overview of the randomised trials, Lancet 351 (1998) 1451-1467.

[11] B. Fisher, J.P. Costantino, D.L. Wickerham, C.K. Redmond, M. Kavanah, W.M. Cronin, V. Vogel, A. Robidoux, N. Dimitrov, J. Atkins, M. Daly, S. Wieand, E. Tan-Chiu, L. Ford, N. Wolmark, Tamoxifen for prevention of breast cancer: Report of the National Surgical Adjuvant Breast and

Bowel Project P-1 study, J. Natl. Cancer Inst. 90 (1998) 1371-1388.

[12] T.L. Wang, Q.D. You, F.S.G. Huang, H. Xiang, Recent Advances in Selective Estrogen Receptor Modulators for Breast Cancer, Mini-Rev. Med. Chem. 9 (2009) 1191-1201.

[13] J.A. Katzenellenbogen, The 2010 Philip S. Portoghese Medicinal Chemistry Lectureship: addressing the "core issue" in the design of estrogen receptor ligands, J. Med. Chem. 54 (2011) 5271-5282.

[14] B.E. Fink, D.S. Mortensen, S.R. Stauffer, Z.D. Aron, J.A. Katzenellenbogen, Novel structural templates for estrogen-receptor ligands and prospects for combinatorial synthesis of estrogens, Chem. Biol, 6 (1999) 205-219.

[15] H.B. Zhou, J.S. Comninos, F. Stossi, B.S. Katzenellenbogen, J.A. Katzenellenbogen, Synthesis and evaluation of estrogen receptor ligands with bridged oxabicyclic cores containing a diarylethylene motif: Estrogen antagonists of unusual structure, J. Med. Chem. 48 (2005) 7261-7274.

[16] K. Ohta, T. Ogawa, A. Kaise, Y. Endo, Novel estrogen receptor (ER) modulators containing various hydrophobic bent-core structures, Bioorgan. Med. Chem. 22 (2014) 3508-3514.

[17] F.E. Vanleeuwen, J. Benraadt, J.W.W. Coebergh, L.A.L.M. Kiemeney, C.H.F. Gimbrere, R. Otter, L.J. Schouten, R.A.M. Damhuis, M. Bontenbal, F.W. Diepenhorst, A.W. Vandenbeltdusebout, H. Vantinteren, Risk of Endometrial Cancer after Tamoxifen Treatment of Breast-Cancer, Lancet 343 (1994) 448-452.

[18] R. Clarke, M.C. Liu, K.B. Bouker, Z.P. Gu, R.Y. Lee, Y.L. Zhu, T.C. Skaar, B. Gomez, K. O'Brien, Y. Wang, L. Hilakivi-Clarke, Antiestrogen resistance in breast cancer and the role of estrogen receptor signaling, Oncogene 22 (2003) 7316-7339.

[19] A. Ring, M. Dowsett, Mechanisms of tamoxifen resistance, Endocr-Relat. Cancer 11 (2004) 643-658.

[20] R. Morphy, Z. Rankovic, Designed multiple ligands. An emerging drug discovery paradigm, J. Med. Chem. 48 (2005) 6523-6543.

[21] N.M. O'Boyle, M.J. Meegan, Designed multiple ligands for cancer therapy, Curr. Med. Chem. 18 (2011) 4722-4737.

[22] W. Lv, J. Liu, T.C. Skaar, D.A. Flockhart, M. Cushman, Design and synthesis of norendoxifen analogues with dual aromatase inhibitory and estrogen receptor modulatory activities, J. Med. Chem. 58 (2015) 2623-2648.

[23] C. Tang, C. Li, S. Zhang, Z. Hu, J. Wu, C. Dong, J. Huang, H.B. Zhou, Novel Bioactive Hybrid Compound Dual Targeting Estrogen Receptor and Histone Deacetylase for the Treatment of Breast Cancer, J. Med. Chem. 58 (2015) 4550-4572.

[24] N.M. O'Boyle, J.K. Pollock, M. Carr, A.J. Knox, S.M. Nathwani, S. Wang, L. Caboni, D.M. Zisterer, M.J. Meegan, beta-Lactam estrogen receptor antagonists and a dual-targeting estrogen receptor/tubulin ligand, J. Med. Chem. 57 (2014) 9370-9382.

[25] Z.C. Tang, S.X. Niu, F. Liu, K.J. Lao, J.S. Miao, J.Z. Ji, X. Wang, M. Yan, L.Y. Zhang, Q.D. You, H. Xiao, H. Xiang, Synthesis and biological evaluation of 2,3-diaryl isoquinolinone derivatives as anti-breast cancer agents targeting ER alpha and VEGFR-2, Bioorg. Med. Chem. Lett. 24 (2014) 2129-2133.

[26] D.J. Hicklin, L.M. Ellis, Role of the vascular endothelial growth factor pathway in tumor growth and angiogenesis, J. Clin. Oncol. 23 (2005) 1011-1027.

[27] M.E. Fratto, M. Imperatori, B. Vincenzi, F. Tomao, D. Santini, G. Tonini, New perspectives: role

of Sunitinib in Breast Cancer, Clin. Ter. 161 (2010) 475-482.

[28] R.R. Patel, S. Sengupta, H.R. Kim, A.J. Klein-Szanto, J.R. Pyle, F. Zhu, T.Y. Li, E.A. Ross, S. Oseni, J. Fargnoli, V.C. Jordan, Experimental treatment of oestrogen receptor (ER) positive breast cancer with tamoxifen and brivanib alaninate, a VEGFR-2/FGFR-1 kinase inhibitor: A potential clinical application of angiogenesis inhibitors, Eur. J. Cancer 46 (2010) 1537-1553.

[29] J.M.W. Gee, J.F.R. Robertson, I.O. Ellis, R.I. Nicholson, Phosphorylation of ERK1/2 mitogen-activated protein kinase is associated with poor response to anti-hormonal therapy and decreased patient survival in clinical breast cancer, Int. J. Cancer 95 (2001) 247-254.

[30] Z. Madak-Erdogan, M. Lupien, F. Stossi, M. Brown, B.S. Katzenellenbogen, Genomic collaboration of estrogen receptor alpha and extracellular signal-regulated kinase 2 in regulating gene and proliferation programs, Mol. Cell. Biol. 31 (2011) 226-236.

[31] L.M. McGlynn, T. Kirkegaard, J. Edwards, S. Tovey, D. Cameron, C. Twelves, J.M. Bartlett, T.G. Cooke, Ras/Raf-1/MAPK pathway mediates response to tamoxifen but not chemotherapy in breast cancer patients, Clin. Cancer Res. 15 (2009) 1487-1495.

[32] R.A. Hill, S. Rudra, B. Peng, D.S. Roane, J.K. Bounds, Y. Zhang, A. Adloo, T.S. Lu, Hydroxyl-substituted sulfonylureas as potent inhibitors of specific [H-3]glyburide binding to rat brain synaptosomes, Bioorgan. Med. Chem. 11 (2003) 2099-2113.

[33] J. Azizian, A.A. Mohammadi, A.R. Karimi, M.R. Mohammadizadeh, A stereoselective three-component reaction: $KAl(SO_4)_2 \cdot 12H_2O$, an efficient and reusable catalyst for the one-pot synthesis of cis-isoquinolonic acids, J. Org. Chem. 70 (2005) 350-352.

[34] G.M. Anstead, K.E. Carlson, J.A. Katzenellenbogen, The estradiol pharmacophore: ligand structure-estrogen receptor binding affinity relationships and a model for the receptor binding site, Steroids 62 (1997) 268-303.

[35] L. Santarpia, S.M. Lippman, A.K. El-Naggar, Targeting the MAPK-RAS-RAF signaling pathway in cancer therapy, Expert Opin. Ther. Tar. 16 (2012) 103-119.

Captions for figures，schemes and tables：

Captions for figures：

Figure 1. Estrogen receptor ligands: (1) Tamoxifen; (2) Raloxifene; (3) PPT; (4) OBHS; (5) *m*-carborane SERM.

Figure 2. Multiple ligands targeting ER.

Figure 3. 21c inhibits the phosphorylation of VEGFR-2 in HUVEC cells. Expression of p-VEGFR-2 and VEGFR-2 in HUVEC cells were examined by western blots. Densitometric analysis was performed to determine the phosphorylation rate of VEGFR-2. Values are mean ±SD (n=3). * $P < 0.05$, ** $P < 0.01$, *** $P < 0.001$ vs. Control group.

Figure 4. The increased mRNA expression of PgR induced by E2 was reversed by **21c** in MCF-7 cells. The mRNA expression of PgR was examined by Real-time PCR. Values are mean ±SD (n=5). * $P < 0.05$, ** $P < 0.01$, *** $P < 0.001$ vs. E2 group. $^{\#}P < 0.05$, $^{\#\#}P < 0.01$, $^{\#\#\#}P < 0.001$.

Figure 5. 21c inhibits the phosphorylation of VEGFR-2 in MCF-7 cells. (A) Expression of p-VEGFR-2 and VEGFR-2 in MCF-7 cells were examined by western blots. (B) Densitometric analysis was performed to determine the phosphorylation rate of VEGFR-2. Values are mean ±SD (n=3). * $P < 0.05$, ** $P < 0.01$, *** $P < 0.001$ vs. Control group.

Figure 6. 21c inhibits the activity of the Raf-1/ERK pathway in MCF-7 cells. (A) Expression of p-Raf-1, Raf-1, p-ERK1/2, and ERK1/2 were examined by western blots in MCF-7 cells. (B) Densitometric analysis was performed to determine the phosphorylation rate of Raf-1 and ERK1/2 . Values are mean ±SD (n=3). * $P < 0.05$, ** $P < 0.01$, *** $P < 0.001$ vs. Control group; $^{\#}P < 0.05$, $^{\#\#}P < 0.01$, $^{\#\#\#}P < 0.001$ vs. Control group.

Figure 7. (A) Predicted binding mode of **21c** within the LBD of ERα (PDB ID: 3ERT). (B) Binding mode of 4-OH-Tamoxifen within the LBD of ERα (PDB ID: 3ERT). (C) Predicted binding mode of **21c** within the LBD of VEGFR-2 (PDB ID: 1YWN).

Captions for schemes：

Scheme 1. Synthesis of compound **12**. Reagents and conditions: (a) Chloral hydrate, conc. H_2SO_4, rt, 12h, 83.6 %; (b) Zn, HOAc, rt, 30min; 93.6% (c) Conc. H_2SO_4, rt, 30min, 90%.

Scheme 2. Synthesis of **18**. Reagents and conditions: (d) acetic anhydride, toluene, reflux, 4h, 100%; (e) ethanol, reflux, 10h, 96.9%; (f) $KAl(SO_4)_2 \cdot 12H_2O$, acetonitrile, rt, 8h, 45.9%; (g) 1) $SOCl_2$, toluene, reflux, 2h; 2) $AlCl_3$, CH_2Cl_2, rt, 10h, 86.7%.

Scheme 3. Synthesis of **19a-f**, **20a-f** and **21a-f**. Reagents and conditions: (h) RCH_2CH_2Cl or $RCH_2CH_2CH_2Cl$, 20% sodium hydroxide, TBAB, THF, reflux, 4h, 37-72%; (i) BBr_3, CH_2Cl_2, rt, 3h, 49-63%.

Captions for tables:

Table 1. Structures of designed compounds

Table 2 Binding affinity of synthesized compounds for ERα

Table 3 Cancer cells antiproliferative activity (IC_{50}, μM)

Table 4 Antiangiogenic activity on VEGFR-2 and HUVEC

Research Highlights

- Designed multiple ligands may exert improved efficacy with lower incidence of side effects.
- A series of 6-aryl-indenoisoquinolone derivatives were described as dual ERα and VEGFR-2 inhibitors.
- Compound 21c turned out to be a promising dual targeting candidate for breast cancer.